

# Helium accreting CO white dwarfs with rotation: helium novae instead of double detonation

S.-C. Yoon and N. Langer

Astronomical Institute, Utrecht University, Princetonplein 5, NL-3584 CC, Utrecht, The Netherlands

Received / Accepted

**Abstract.** We present evolutionary models of helium accreting carbon-oxygen white dwarfs in which we include the effects of the spin-up of the accreting star induced by angular momentum accretion, rotationally induced chemical mixing and rotational energy dissipation. Initial masses of  $0.6 M_{\odot}$  and  $0.8 M_{\odot}$  and constant accretion rates of a few times  $10^{-8} M_{\odot}/\text{yr}$  of helium rich matter have been considered, which is typical for the sub-Chandrasekhar mass progenitor scenario for Type Ia supernovae. It is found that the helium envelope in an accreting white dwarf is heated efficiently by friction in the differentially rotating spun-up layers. As a result, helium ignites much earlier and under much less degenerate conditions compared to the corresponding non-rotating case. Consequently, a helium detonation may be avoided, which questions the sub-Chandrasekhar mass progenitor scenario for Type Ia supernovae. We discuss implications of our results for the evolution of helium star plus white dwarf binary systems as possible progenitors of recurrent helium novae.

**Key words.** stars: evolution – stars: white dwarf – stars: rotation – stars:novae – supernovae: Type Ia

## 1. Introduction

Type Ia supernovae are of key importance for the chemical evolution of galaxies, as they are a major producer of iron group elements (e.g. Nomoto et al. 1984; Renzini 1999). They were also found to be excellent distance indicator and have become an indispensable tool in cosmology (Phillips 1993; Hamuy et al. 1996; Branch 1998). The recent suggestion of a non-zero cosmological constant is partly based on observations of SNe Ia at high redshift (Leibundgut 2001). Given that distance determinations at high redshift through SNe Ia depend on the assumption of the homogeneity of SNe Ia light curves throughout the ages, an understanding of the possible diversity of their progenitors is crucial to evaluate this approach. Nevertheless, the progenitors of Type Ia supernovae have not been identified yet, and the debate on their exact nature continues (e.g., Livio 2001).

One possibility to obtain a SN Ia is the detonation of the degenerate helium layer accumulated on top of a CO white dwarf due to mass transfer from its low mass helium star companion in a close binary system, which triggers a carbon detonation in the white dwarf core. This is the so called double detonation or sub-Chandrasekhar mass scenario for SNe Ia, as it may allow to explode white dwarfs with masses well below the Chandrasekhar mass (e.g. Nomoto 1982; Fujimoto 1982; Limongi & Tornambé 1991; Livne 1990; Woosley & Weaver 1994; Livne & Arnett 1995). While the

capability of the helium detonation to ignite the CO core is still debated (e.g., Livio 2001), the helium detonation by itself would produce an explosion of supernova scale.

Currently, the sub-Chandrasekhar mass scenario is not favored as a major source of SNe Ia mainly because the light curves and spectra obtained from this model are not in good agreement with observations (e.g. Höflich & Khokhlov 1996; Nugent et al. 1997). Especially, the predicted presence of high velocity Ni and He is most stringently criticized (e.g. Hillebrandt & Niemeyer 2000; Livio 2001).

On the other hand, stellar and binary evolution theory predicts a realization frequency of binary systems such as helium star cataclysmics — which might produce double detonating sub-Chandrasekhar mass white dwarfs — which amounts to a few times  $10^{-3} \text{ yr}^{-1}$  per galaxy (e.g. Iben & Tutukov 1991; Regös et al. 2002) which is comparable to the expected total SN Ia rate in the Milky Way. This raises the question why such explosions are practically never observed.

We note that the sub-Chandrasekhar mass SN progenitor models which have been constructed so far neglected the effects of rotation, which can be one of the primary factors determining the evolution of stars, in particular of massive stars (Langer 1998; Maeder & Meynet 2000). Iben & Tutukov (1991) pointed out that rotation may indeed be important in helium star cataclysmic systems. Yoon & Langer (2002, 2004) and Yoon et al. (2004) showed that effects of rotation might be essential for the evolution of accreting white dwarfs when the accreted matter contains a high specific angular momentum. The induced spin-up was found to change the white

dwarf structure significantly and to produce rotationally induced chemical mixing.

In this paper, we suggest that rotation could play a key role in helium accreting white dwarfs such that in model which would produce a helium detonation this phenomenon is completely avoided when the white dwarf spin-up is considered. After explaining the numerical method and physical assumptions of the present study in Sect. 2, we investigate the evolution of helium accreting carbon-oxygen white dwarfs with accretion rates of  $\sim 10^{-8} M_{\odot}/\text{yr}$ , with the effects of rotation considered, in Sect. 3. Implications of our results for helium novae and neutron capture nucleosynthesis are discussed in Sect. 4. Our main conclusions are summarized in Sect. 5

## 2. Numerical method and physical assumptions

We have computed the numerical models with a hydrodynamic stellar evolution code (Langer et al. 1988), which incorporates the effect of the centrifugal force on the stellar structure and rotationally induced transport of angular momentum and chemical species due to the dynamical and secular shear instability, the Goldreich-Schubert-Fricke instability and the Eddington-Sweet circulations (Heger et al. 2000; Yoon & Langer 2004). Conservation of angular momentum and energy of viscous fluids requires dissipation of rotational energy as angular momentum is transported by viscous friction in differentially rotating layers (e.g. Landau & Lifshitz 1984). This effect is considered in our calculations following Mochkovitch & Livio (1989) as:

$$\epsilon_{\text{diss,r}} = \frac{1}{2} \nu_{\text{turb}} \left( \frac{\partial \omega}{\partial \ln r} \right)^2 \quad (\text{erg g}^{-1} \text{sec}^{-1}), \quad (1)$$

where  $\omega$  is the angular velocity,  $r$  the radius and  $\nu_{\text{turb}}$  the turbulent viscosity due to the above mentioned rotationally induced instabilities (Heger et al. 2000; Yoon & Langer 2004).

Nuclear networks for the changes in chemical composition and the nuclear energy generation include more than 60 reactions (see Heger et al. 2000 for more details). In particular, the  $^{14}\text{N}(e^-, \nu)^{14}\text{C}(\alpha, \gamma)^{18}\text{O}$  reaction (hereafter NCO reaction), which becomes active when  $\rho \gtrsim 10^6 \text{ g/cm}^3$  (Hashimoto et al. 1984), has been newly included for this study. We have used the  $^{14}\text{N}(e^-, \nu)^{14}\text{C}$  reaction rate given by Martinez (2002, Private communication) and followed Caughlan and Fowler (1988) for the  $^{14}\text{C}(\alpha, \gamma)^{18}\text{O}$  reaction rate. The accretion induced heating is described following Neo et al. (1977), and the accreted matter is assumed to have the same entropy as that of the surface of the accreting star.

Two initial masses, 0.6 and 0.8  $M_{\odot}$ , are considered for the CO white dwarf models. Since isolated white dwarfs are generally found to rotate with a surface velocity of  $v_s \lesssim 40 \text{ km/s}$  (Heber et al. 1997; Koester et al. 1998; Kawaler 2003), the initial rotation velocity of our models is assumed to be as slow as 10 km/s at the white dwarf equator (see also Langer et al. 1999). Other physical properties of the white dwarf initial models are summarized in Table 1. While most of our simulations start with a cold white dwarf with  $\log L_s/L_{\odot} \simeq -2.0$ , an initially hot white dwarf with  $\log L_s/L_{\odot} \simeq 2.508$  is also considered for one model sequence (TC, Table 2; cf. Sect. 4.1). The

**Table 1.** Physical quantities of the initial white dwarf models: mass, surface luminosity, central temperature, central density, radius and rotation velocity. The hot white dwarf model in the third row is only used for sequence TC (see Table 2).

$M_{\text{WD,init}}$ $M_{\odot}$	$\log L_{s,\text{init}}/L_{\odot}$	$T_{c,\text{init}}$ $10^7 \text{ K}$	$\rho_{c,\text{init}}$ $10^6 \text{ g/cm}^3$	$R_{\text{WD,init}}$ $R_{\odot}$	$v_{\text{rot,init}}$ $\text{km/s}$
0.6	-2.049	1.69	3.64	0.0126	10
0.8	-2.024	1.59	10.7	0.0101	10
0.8	2.508	14.4	6.44	0.0186	10

accreted matter, received with two different constant accretion rates of  $\dot{M} = 2 \times 10^{-8}$  and  $3 \times 10^{-8} M_{\odot}/\text{yr}$ , is assumed to have  $Y = 0.982$  and  $X_{\text{N}} = 0.012$ , where  $Y$  and  $X_{\text{N}}$  are the mass fraction of helium and nitrogen, respectively.

In a close binary system, the white dwarf is believed to receive matter through a Keplerian accretion disk if its magnetic field is not considerable. The accreted matter may thus carry an amount of specific angular momentum which corresponds to critical rotation at the white dwarf equator. However, continuous angular momentum gain under these conditions leads to over-critical rotation soon after the onset of mass transfer in the outer part of the accreting star (Yoon & Langer 2002). Therefore, we limit the angular momentum gain such that the accreting star may not rotate over-critically, as follows:

$$j_{\text{acc}} = \begin{cases} f \cdot j_{\text{Kepler}} & \text{if } v_s < f \cdot v_{\text{Kepler}} \\ 0 & \text{if } v_s = f \cdot v_{\text{Kepler}} \end{cases} \quad (2)$$

where  $v_s$  denotes the surface velocity at the white dwarf equator,  $j_{\text{acc}}$  the specific angular momentum of the accreted matter, and  $v_{\text{Kepler}}$  and  $j_{\text{Kep}}$  the Keplerian value of the surface velocity and the specific angular momentum at the white dwarf equator, respectively. The dimensionless parameter  $f$  represents the fraction of the Keplerian value of the specific angular momentum which is contained in the accreted matter, and also the maximum fraction of the critical rotational velocity with which the white dwarf equator may rotate.

The use of  $f = 1$  might be the most natural choice to describe the realistic situation, as Paczyński (1991) and Popham & Narayan (1991) argue that a critically rotating star may continue to accrete matter from a Keplerian disk by transporting angular momentum from the star back into the disk due to turbulent viscosity. However, as the correct treatment of close-to-critical rotation is beyond the capabilities of our numerical code, we also consider the case  $f < 1$ . As discussed in Yoon & Langer (2004), the correction factors of  $f_{\text{P}}$  and  $f_{\text{T}}$  which are included in the stellar structure equations for describing the effects of rotation (cf. Heger et al. 2000) are limited to 0.75 and 0.95, respectively. This limit corresponds to a rotation rate of about 60% of critical rotation, up to which our one dimensional approximation in computing the effective gravitation potential can accurately describe the structure of the rotating star. In our models with  $f = 1$ , where the outer envelope rotates close to critically, the centrifugal force is accordingly underestimated. Although the region which rotates faster than 60% critical contains only little mass (see Sect. 3), we also consider the case

**Table 2.** Properties of the computed model sequences.  $M_{\text{WD,init}}$  : initial mass,  $\dot{M}$  : accretion rate,  $f$  : fraction of the Keplerian value of the accreted specific angular momentum (see Eq. 2).  $\dot{E}_{\text{diss}}$  : Rotational energy dissipation due to frictional heating. Yes (or No) means that this effect is considered (or not).  $\Delta M_{\text{He}}$  : accumulated helium mass until the helium ignition point.  $T_c$  and  $\rho_c$  : central temperature and density in the last computed model.  $T_{\text{He}}$  : maximum temperature in the helium envelope in the last computed model.  $\rho_{\text{He}}$  and  $\eta_{\text{He}}$  : density and degeneracy parameter at the position of the maximum temperature in the helium envelope in the last computed model. The last column indicates whether the model sequence will finally result in helium detonation or not.

No.	$M_{\text{WD,init}}$ $M_{\odot}$	$\dot{M}$ $10^{-8} M_{\odot}/\text{yr}$	$f$	$\dot{E}_{\text{diss}}$	$\Delta M_{\text{He}}$ $M_{\odot}$	$T_c$ $10^8 \text{ K}$	$\rho_c$ $10^6 \text{ g/cm}^3$	$T_{\text{He}}$ $10^8 \text{ K}$	$\rho_{\text{He}}$ $10^6 \text{ g/cm}^3$	$\eta_{\text{He}}$	Detonation?
N1	0.6	2.0	–	–	0.229	0.60	10.9	2.0	1.48	11	Yes
N2	0.6	3.0	–	–	0.185	0.54	8.8	1.4	0.55	9	No
N3	0.8	2.0	–	–	0.168	0.55	26.1	2.0	1.58	13	Yes
N4	0.8	3.0	–	–	0.150	0.46	23.6	1.2	1.50	19	Yes
R1	0.6	2.0	1.0	Yes	0.080	0.39	4.4	1.2	0.22	6	No
R2	0.6	3.0	1.0	Yes	0.061	0.23	4.2	1.4	0.15	4	No
R3	0.8	2.0	1.0	Yes	0.022	0.14	11.0	1.5	0.15	4	No
R4	0.8	3.0	1.0	Yes	0.017	0.14	10.6	3.8	0.03	0.3	No
TA1	0.6	2.0	0.6	Yes	0.149	0.50	5.97	1.2	0.42	9	No
TA2	0.6	3.0	0.6	Yes	0.106	0.45	4.70	3.5	0.16	2	No
TA3	0.8	2.0	0.6	Yes	0.073	0.21	14.2	1.3	0.38	8	No
TA4	0.8	3.0	0.6	Yes	0.045	0.18	12.7	1.4	0.28	6	No
TB1	0.6	2.0	1.0	No	0.402	0.59	9.6	1.1	1.14	22	Yes
TB3	0.8	2.0	1.0	No	0.233	0.65	21.3	1.2	1.36	21	Yes
TC	0.8	1.0	1.0	Yes	0.002	0.95	8.5	2.8	0.001	0.06	No

$f = 0.6$ , apart from the case  $f = 1.0$ . With  $f = 0.6$ , the white dwarf never rotates faster than 60 % of the Keplerian value, and thus the stellar structure is accurately described throughout the white dwarf interior.

For comparison, we also compute rotating models where the rotational energy dissipation is neglected, as well as non-rotating models, with otherwise identical initial conditions. In Table 2 we list all computed model sequences. The index N in the model number indicates a non-rotating model sequence, while R denotes a rotating one with  $f = 1.0$ . The index TA is for rotating test models with  $f = 0.6$ , while TB is used for rotating test models with  $f = 1.0$  without rotational energy dissipation (i.e.,  $\epsilon_{\text{diss,r}} = 0.0$ ). The sequence TC designates the only model starting with a hot white dwarf. All sequences are computed up to the point where the accumulated helium shell ignites.

### 3. Results

We summarize the results of our simulations in Table 2. Here,  $T_{\text{He}}$ ,  $\rho_{\text{He}}$  and  $\eta_{\text{He}}$  denote, for the last computed model, the maximum temperature in the helium envelope and the corresponding density and the degeneracy parameter ( $\psi/kT$ , e.g. Kippenhahn & Weigert 1990).  $\Delta M_{\text{He}}$  gives the accumulated helium mass until helium ignition.

At helium ignition we stop our calculations, and our models are per se not able to predict whether the helium burning develops into a helium detonation or not. However, from the literature (e.g., Woosley & Weaver 1994) we conclude that a helium detonation can not develop if the ignition density is smaller than  $\sim 10^6 \text{ g/cm}^3$ , due to the quenching of the thermonuclear runaway by expansion. For  $\rho_{\text{He}} < 10^6 \text{ g/cm}^3$ , therefore, the

helium ignition may result only in a nova-like shell flash, which will not be able to trigger core carbon ignition.

Our results for the non-rotating model sequences are found in good agreement with similar models computed by Woosley & Weaver (1994) and Piersanti et al. (2001). For instance, for a sequence with the same initial mass and accretion rate as for our sequence N1, Piersanti et al. obtained  $\Delta M_{\text{He}} = 0.244 M_{\odot}$ , which does not differ much from our result of  $\Delta M_{\text{He}} = 0.229 M_{\odot}$ . The slightly smaller value of the present study may be attributed to a small difference in the initial nitrogen mass fraction, which triggers the NCO reaction when  $\rho_c \gtrsim 10^6 \text{ g/cm}^3$  and initiates helium burning.

Fig. 1 illustrates the evolution of our white dwarf models with  $M_{\text{WD,init}} = 0.8 M_{\odot}$  and  $\dot{M} = 2 \times 10^{-8} M_{\odot}/\text{yr}$  (sequences N3, R3 and TB3). In the non-rotating case, the temperature of the helium envelope continues to increase due to accretion induced heating. When the white dwarf mass reaches about  $0.9 M_{\odot}$ , the density at the bottom of the helium envelope starts exceeding  $10^6 \text{ g/cm}^3$  and the NCO reaction becomes active, accelerating the temperature increase. Finally, helium burning starts when  $M_{\text{WD}}$  reaches  $0.968 M_{\odot}$ . The density at the helium ignition point is about  $1.6 \times 10^6 \text{ g/cm}^3$  and a detonation is likely to follow.

The evolution of the corresponding rotating model (R3) in Fig. 1 looks similar, but helium ignites much earlier than in the non-rotating case. The maximum temperature in the helium envelope reaches  $10^8 \text{ K}$  when  $M_{\text{WD}} \simeq 0.818 M_{\odot}$ . Helium burning develops quickly thereafter, and the nuclear energy generation amounts to  $\log L_{\text{He}}/L_{\odot} \simeq 5.0$  when  $M_{\text{WD}} \simeq 0.822 M_{\odot}$ . Only  $0.022 M_{\odot}$  of helium has been accumulated by then, which is about 10 times less than in the non-rotating case.

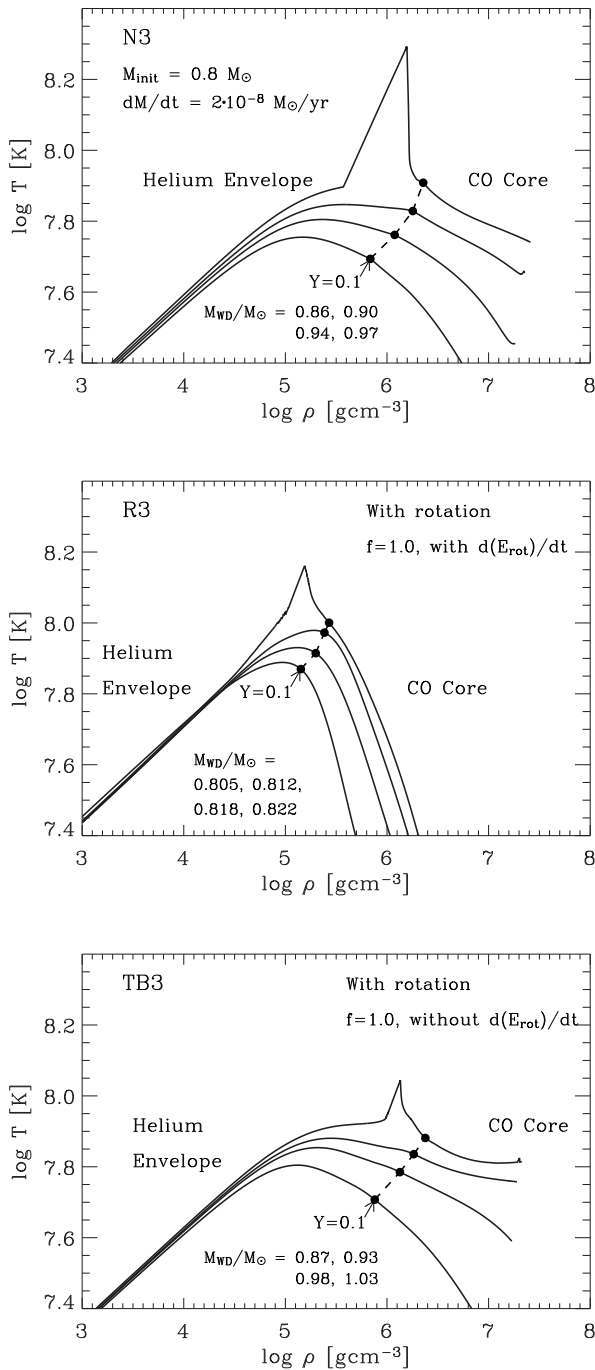


**Fig. 1.** Evolution of accreting white dwarf models of sequence N3, R3 & TB3, for which  $M_{\text{WD,init}} = 0.8 M_{\odot}$  and  $\dot{M} = 2 \times 10^{-8} M_{\odot}/\text{yr}$ , in the  $\log \rho - \log T$  plane. The boundary between the CO core and the helium envelope, defined through  $Y = 0.1$ , is indicated by a filled circle for each model.

Importantly, the ignition density  $\rho_{\text{He}}$  is also found about 10 times lower ( $1.5 \times 10^5 \text{ g/cm}^3$ ) than in the non-rotating case, implying that a helium detonation may be avoided.

The reason for the early helium ignition in the rotating sequence is as follows. As explained above, the white dwarf obtains angular momentum carried by the accreted matter. The

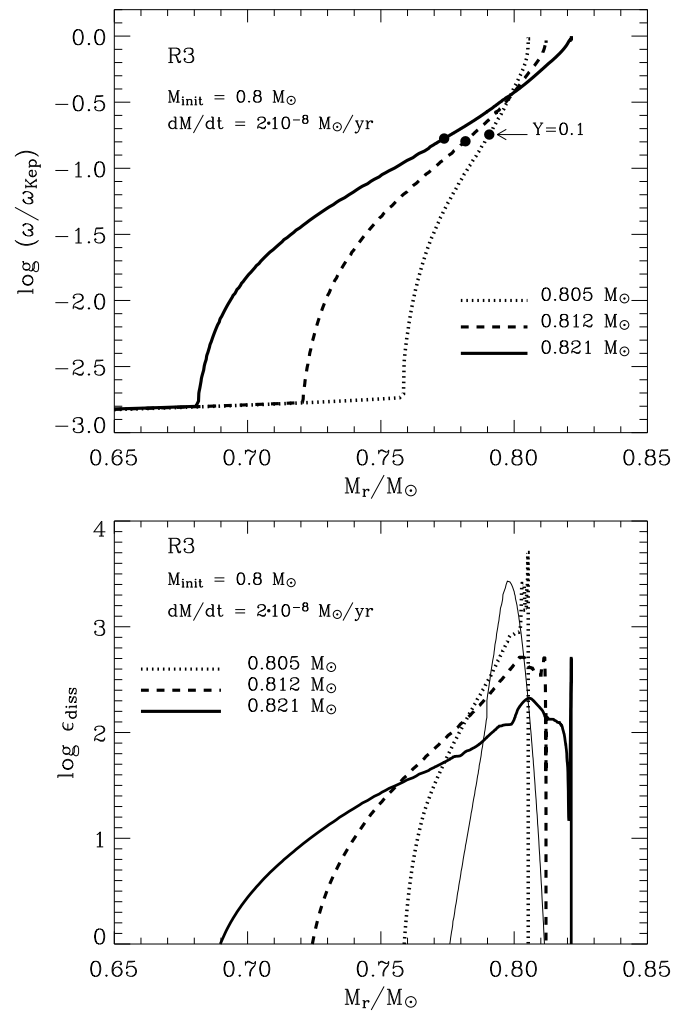


**Fig. 2.** Upper panel: Angular velocity in units of the local Keplerian value as function of the mass coordinate in model sequence R3 when  $M_{\text{WD}} = 0.805, 0.812$  and  $0.821 M_{\odot}$ . The filled circles indicate the boundary of the CO core and helium envelope, as defined in Fig. 1, where the helium mass fraction is 0.1. Lower panel: Rotational energy dissipation due to friction (Eq. 1) at the same evolutionary epochs as in the upper panel. The thin solid line denotes the energy generation rate due to nuclear reactions when  $M_{\text{WD}} = 0.821 M_{\odot}$ .

angular momentum is thus transported from the surface into the interior by various rotationally induced hydrodynamic instabilities. In our white dwarf models, Eddington Sweet circulation, the secular shear and the GSF instability dominate in the non-degenerate envelope, while the dynamical shear instability is most important in the degenerate interior, as discussed in detail by Yoon & Langer (2004). The white dwarf interior is spun up progressively with time, giving rise to rotational energy dissipation as shown in Fig. 2. In the upper panel of the figure, the angular velocity reveals a strong degree of differential rotation. The consequent energy dissipation rate is given in the lower panel in the same figure. The total energy dissipation rate integrated over the spun-up layers in the given models amounts to  $8.8 L_{\odot}$ ,  $6.2 L_{\odot}$ , and  $3.6 L_{\odot}$  for  $M_{\text{WD}} = 0.805 M_{\odot}$ ,

0.812  $M_{\odot}$ , and 0.821  $M_{\odot}$  respectively. Together with the accretion induced heating, this additional energy supply speeds up the temperature increase in the helium envelope, leading to the earlier helium ignition compared to the non-rotating case.

For comparison, the white dwarf evolution in sequence TB3, where the rotational energy dissipation is neglected while everything else is as in sequence R3, is shown in the third panel of Fig. 1. In this case, helium ignition occurs even later than in the corresponding non-rotating case (N3). This is due to the lifting effect of the centrifugal force, which reduces the accretion induced heating. The density at the bottom of the helium envelope when the helium burning is induced by the NCO reaction is about  $1.36 \times 10^6 \text{ g/cm}^3$ , implying that a helium detonation might be triggered in this case.

As shown in Fig. 2, the surface layers of the white dwarf models in sequence R3, where  $f = 1$  is used, rotate faster than 60 % critical, above which the effects of rotation are underestimated by our computational method. In the models with  $M_{\text{WD,init}} = 0.8 M_{\odot}$ , i.e., in sequences R3 and R4, however, this fast rotating region is limited to only 1% of the white dwarf mass, which is not likely to affect the result significantly. On the other hand, about 7% in mass, which include a significant fraction of the helium envelope, exceed the limit at helium ignition in model sequences R1 and R2, for which  $M_{\text{WD,init}} = 0.6 M_{\odot}$  and  $f = 1$  are adopted. Nevertheless, results from the corresponding sequences with  $f = 0.6$  (TA1, TA2, TA3 and TA4), where the white dwarf models are forced to rotate below 60% critical throughout the white dwarf interior, lead us to the same conclusion as in case of  $f = 1$ : helium ignites at such a low density (even though it is somewhat higher than in case of  $f = 1$ ) that a supernova event is unlikely to occur. For instance, in model sequence TA1, we have  $\rho_{\text{He}} = 4.2 \times 10^5 \text{ g/cm}^3$  when the maximum temperature reaches  $1.2 \times 10^8 \text{ K}$ . This is about 3.5 times lower than in the corresponding non-rotating case ( $\rho_{\text{He}} = 1.48 \times 10^6 \text{ g/cm}^3$ ) and about two times higher than in case of  $f = 1$  ( $\rho_{\text{He}} = 2.2 \times 10^5 \text{ g/cm}^3$ ).

## 4. Discussion

### 4.1. Connection to recurrent helium novae

As discussed by Iben & Tutukov (1991) and Limongi & Tornambé (1991), a relatively low helium accretion rate of  $\sim 10^{-8} M_{\odot}/\text{yr}$  onto a CO white dwarf can be realized, for example, in binary systems which consist of a  $0.6 \dots 1.0 M_{\odot}$  CO white dwarf and a less massive helium star. Mass transfer in such binary systems is driven by gravitational wave radiation, and the resulting mass transfer rate is found to be insensitive to the exact masses of white dwarf and helium star, at a few times  $10^{-8} M_{\odot}/\text{yr}$  (Iben & Tutukov 1991; Limongi & Tornambé 1991). Many of such binary systems, if not all, could produce a supernova which will appear as Type Ia (Taam 1980; Nomoto 1982; Iben & Tutukov 1991; Limongi & Tornambé 1991; Woosley & Weaver 1994; Livne & Arnett 1995), while the resulting light curves and spectra may be abnormal (Höflich & Tutukov 1996; Nugent et al. 1997). As mentioned in the introduction of this paper, binary population synthesis models show that the production rate of such

events may be comparable to the observed SN Ia rate (e.g. Iben & Tutukov 1991; Regös et al. 2002), and therefore the apparent absence of such a peculiar type of supernovae has been a puzzling matter.

The results of the present study offer a possible solution to this problem: helium accreting CO white dwarfs with an accretion rate of  $\sim 10^{-8} M_{\odot}/\text{yr}$  may not result in a supernova at all, but may instead produce nova-like explosions. The accumulated helium mass of  $\Delta M_{\text{He}} \simeq 0.02 \dots 0.1 M_{\odot}$  in our rotating models indicates that in a low mass helium star + CO white dwarf binary system, nova explosions will occur recurrently, with a period of about  $10^6 \text{ yr}$ .

As pointed out by Iben & Tutukov (1991), various factors need to be considered for predicting the further evolution of such a binary system after the first nova outburst. First, any mass loss induced by the helium flash will affect the binary orbit. I.e., the nova induced mass loss will widen the orbit and interrupt the mass transfer for some time (Iben & Tutukov 1991). However, the angular momentum loss due to gravitational wave radiation will lead the helium star to fill its Roche lobe soon again (after  $\sim 10^6 \text{ yr}$ ) as discussed below.

Second, the first nova outburst may heat up the white dwarf significantly, and the white dwarf may still be hot when the second mass transfer starts, compared to the case of the first mass transfer. Model sequence TC, where an initially hot white dwarf with  $\log L_s/L_{\odot} = 2.508$  is adopted, was computed in order to investigate the effect of a pre-heated white dwarf. A value of  $\dot{M} = 10^{-8} M_{\odot}/\text{yr}$  for this sequence, which is smaller than in other model sequences, was chosen to consider the decrease of the mass transfer rate due to the change of the orbit as the binary system loses mass via helium nova outbursts (cf. Fig 3). A comparison of  $\Delta M_{\text{He}}$  in sequence TC ( $\Delta M_{\text{He}} \simeq 0.002 M_{\odot}$ ) with the accumulated helium masses in the sequences R3 and R4 ( $\Delta M_{\text{He}} \simeq 0.02 M_{\odot}$ ) implies that  $\Delta M_{\text{He}}$  decreases by more than a factor of 10 if the white dwarf is pre-heated. Therefore, the second and any further helium flash may be much weaker than the first one.

In an attempt to make more detailed conjectures on the evolution and final fate of binary systems of the considered kind, we made a simple experiment as follows. We constructed a binary star model consisting of a zero-age helium main sequence star of  $0.6 M_{\odot}$  and a CO white dwarf of  $0.8 M_{\odot}$  in an 1.08 h orbit ( $A_{\text{orbit,init}} = 0.6 R_{\odot}$ , cf. Limongi & Tornambé 1991). Here, the white dwarf is approximated by a point mass. Since it appears likely that the accreted helium will be ejected from the system by the violent helium shell flash when about  $0.02 M_{\odot}$  of helium is accumulated as implied by the results of sequences R3 and R4, we assume this for the evolution of our binary system. As discussed above, the subsequent helium flashes may occur with a smaller  $\Delta M_{\text{He}}$ . Therefore, for the subsequent evolution the white dwarf is assumed to lose the accumulated matter at every time when  $\Delta M_{\text{He}} = 0.002 M_{\odot}$  is achieved. For comparison, a second binary evolution model with the same initial condition is calculated, with the assumption of no mass loss due to helium flashes. The evolution of the helium star and the change of the binary orbit due to the mass transfer, stellar wind mass loss and gravitational wave radiation are followed

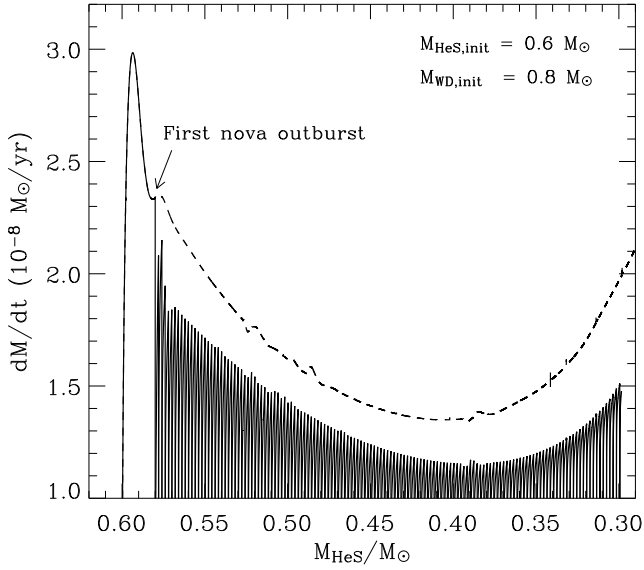


**Fig. 3.** Mass transfer rate as function of the helium star mass, for a binary system consisting initially of an  $0.6 M_{\odot}$  helium star and an  $0.8 M_{\odot}$  CO white dwarf (the latter here being approximated by a point mass). Mass transfer is initiated by gravitational wave radiation. The solid line illustrates the case where mass loss due to helium flashes is considered, while the dashed line was computed assuming that no mass loss occurs.

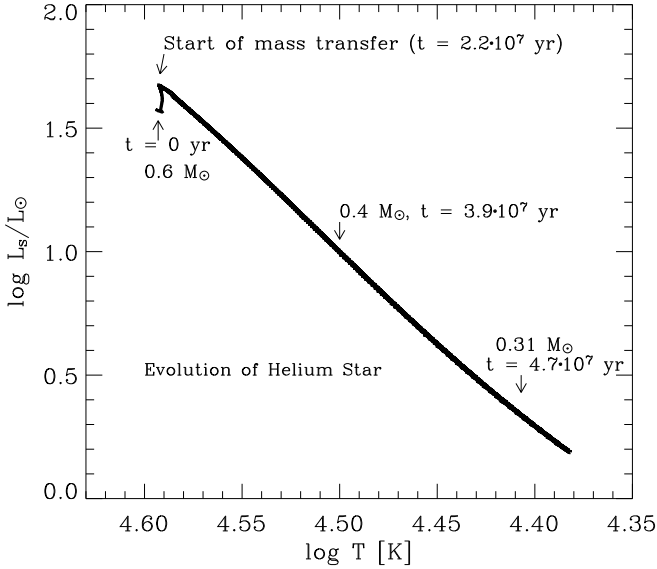


**Fig. 4.** Evolution in the HR diagram of the helium star (initial mass  $0.6 M_{\odot}$ ) component of the binary system considered in in Fig. 3, for case with nova induced mass loss.

by using a binary stellar evolution code (see Langer et al. 2000 for more details about the code).

Fig. 3 shows the evolution of the mass transfer rate in the considered system, as function of the helium star mass ( $M_{\text{HeS}}$ ). The mass transfer from the helium star starts when the helium mass fraction in the helium star center equals 0.39. The orbital period at this moment is about 39 min. The mass transfer rate

initially increases to  $3 \times 10^{-8} M_{\odot}/\text{yr}$  and has decreased to  $2.3 \times 10^{-8} M_{\odot}/\text{yr}$  by the time  $\Delta M_{\text{He}}$  reaches  $0.02 M_{\odot}$ . As the white dwarf is assumed to lose  $0.02 M_{\odot}$  at this point due to the helium nova flash, the system becomes detached for about  $5.5 \times 10^5$  yr, after which the helium star again fills its Roche lobe. Further-on, the white dwarf loses mass whenever  $\Delta M_{\text{He}}$  reaches  $0.002 M_{\odot}$ , and thus the mass transfer is switched on and off repeatedly every  $\sim 1.5 \times 10^5$  yr. We follow the evolution of the system until the helium star mass decreases to  $0.30 M_{\odot}$ .

Fig. 4 shows the evolution of the helium star in the HR diagram. The helium star luminosity decreases continuously as it loses mass, and it will finally evolve into a white dwarf. At this stage, the binary system will resemble an AM CVn system.

At the end of the calculation (i.e.,  $M_{\text{HeS}} = 0.30 M_{\odot}$ ), the central helium abundance has decreased to 0.16, and more than  $0.1 M_{\odot}$  of helium is still available in the envelope for further mass transfer. Since about 135 nova outbursts occurred until the end of the calculation, more than 180 recurrent nova outbursts in total are expected to occur throughout the evolution of the considered binary system. This implies that helium nova explosions in low mass helium star + CO white dwarf binary systems could be realized with a frequency of  $\sim 0.1 \text{ yr}^{-1}$  in our Galaxy, given that such binary systems are being produced at a frequency of  $\sim 0.001 \text{ yr}^{-1}$  (Iben & Tutukov 1991; Regös et al. 2002). The recently discovered outburst of V445 Puppis, which has been attributed to a helium nova (Ashok & Banerjee 2003; Kato & Hachisu 2003), may be a promising observational counterpart of such an event. The high observed carbon abundance in this system (Ashok & Banerjee 2003) might be explained by the rotationally induced chemical mixing in the accreting white dwarf, the effects of which are discussed in the next section.

#### 4.2. Rotationally induced chemical mixing and neutron capture nucleosynthesis

As already suggested by Iben & Tutukov (1991), strong helium flashes in accreting CO white dwarfs may activate neutron capture nucleosynthesis, since neutrons can be provided via the  $^{22}\text{Ne}(\alpha, n)^{25}\text{Mg}$  reaction. We note that favorable conditions for neutron capture nucleosynthesis might be achieved with rotation compared to the non-rotating case, due to the rotationally induced chemical mixing (cf. Langer et al. 1999).

Fig. 5a gives the mass fraction of  $^4\text{He}$ ,  $^{12}\text{C}$  and  $^{22}\text{Ne}$  in the initial model ( $M_{\text{WD}} = 0.8 M_{\odot}$ ) of sequence R3, as well as in the model with  $M_{\text{WD}} = 0.822 M_{\odot}$ , which is immediate before the helium ignition. It is found that  $^{12}\text{C}$  and  $^{22}\text{Ne}$  have been significantly dredged up into the helium envelope when helium ignites, due to rotationally induced mixing. For instance, comparing the two models shown in Fig. 5a reveals that the mass fraction of  $^{12}\text{C}$  and  $^{22}\text{Ne}$  at  $M_r = 0.8 M_{\odot}$  has increased by about a factor of 10 when helium ignites.

The ignition of helium induces convection. Fig. 5b shows the chemical structure when  $T_{\text{He}}$  reaches  $1.5 \times 10^8$  K. At this point, the convective layer has a mass of  $\Delta M_{\text{conv}} \simeq 0.01 M_{\odot}$ , extending from  $M_r = 0.796 M_{\odot}$  to  $M_r = 0.806 M_{\odot}$ . The

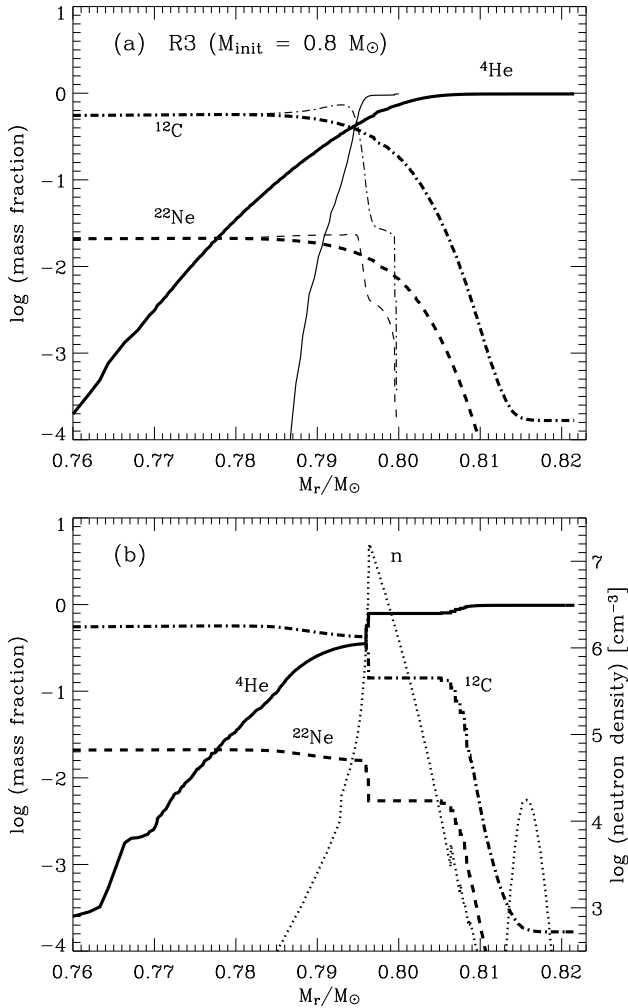


**Fig. 5.** (a) Chemical profiles in the outer layers of the white dwarf models of sequence R3 when  $M_{\text{WD}} = 0.8 M_\odot$  (initial model, thin lines), and  $M_{\text{WD}} = 0.822 M_\odot$  (thick lines) which is immediate before the helium ignition. The solid and dotted-dashed lines give the mass fraction of  $^4\text{He}$  and  $^{12}\text{C}$  respectively, as function of the mass coordinate. The dashed line denotes the mass fraction of  $^{22}\text{Ne}$ . (b) Same as in (a) but after the ignition of helium. The dotted line denotes the neutron density, for which the scale is given at the right side.

abundance of the dredged up core material in the convective layer amounts to 0.15 for  $^{12}\text{C}$  and  $5.5 \times 10^{-3}$  for  $^{22}\text{Ne}$ , respectively. Neutrons are released by the  $^{22}\text{Ne}(\alpha, n)^{25}\text{Mg}$  reaction, and a maximum neutron density of  $\sim 10^7 \text{ cm}^{-3}$  is achieved at  $M_r = 0.76 M_\odot$  in our last model. This neutron density may be somewhat overestimated in our calculation, since we did not include the reaction  $^{14}\text{N}(n, p)^{14}\text{C}$  in our network (cf Siess, Goriely & Langer 2003). However, we note that alpha particles are mixed significantly into the  $^{22}\text{Ne}$ -rich region, and that large amount of neutrons will be released in the further evolution of the flash which is not covered any more by our model, as hydrodynamic effects in the exploding layers may become important. Therefore, we leave the exploration of the neutron capture nucleosynthesis effects in our models for the future.

## 5. Concluding remarks

We have shown that the effects of rotation in helium accreting white dwarfs may be incompatible with the scenario of double detonations in sub-Chandrasekhar mass CO white dwarfs as possible SNe Ia progenitors. In helium accreting white dwarfs, we find the thermal evolution to be affected by viscous heating due to differential rotation in the spun-up layers, such that helium ignition is induced at too low densities to develop a detonation. This may give a plausible solution to the long standing problem of the missing observational counterparts of sub-Chandrasekhar explosions, which are predicted to occur with a frequency comparable to the observed SN Ia rate.

We discussed that binary systems consisting of a CO white dwarf and a less massive helium star may be possible progenitors of recurrent helium novae (Iben & Tutukov 1991), which may be analogous to V445 Puppis (Ashok & Banerjee 2003; Kato & Hachisu 2003). After the first strong helium nova flash in such binary systems, rather mild nova outbursts are expected to occur recurrently with a period of  $\sim 10^5 \text{ yr}$ . The realization frequency of such a helium nova may be as high as  $\sim 0.1 \text{ yr}^{-1}$  in our Galaxy.

Rotation induces chemical mixing of  $^{22}\text{Ne}$  and  $^4\text{He}$  at the bottom of the helium envelope, which may provide interesting conditions for neutron capture nucleosynthesis to occur during the helium nova flashes.

Finally, we note that other important mechanisms for the angular momentum redistribution in white dwarfs may exist than those considered in the present study. In particular, we neglected the possible role of magnetic fields, which may increase the efficiency of the angular momentum transport significantly (cf. Heger et al. 2003; Maeder & Meynet 2003). If the spin-up time scale is shorter than considered in the present study, the resulting shear strength will be weaker and the effect of rotational energy dissipation may not be as important as shown here. However, studies of magnetic effects in accreting white dwarfs have to be left for future investigations.

*Acknowledgements.* We are very grateful to Gabriel Martinez for kindly providing us with a data table of the  $^{14}\text{N}(e^-, \nu)^{14}\text{C}$  reaction rate. We thank Onno Pols for fruitful discussion. This research has been supported in part by the Netherlands Organization for Scientific Research (NWO).

## References

- Ashok, N.M., Banerjee, D.P.K., 2003, A&A, 409, 1007
- Branch, D., 1998, ARA&A, 36, 17
- Caughlan, G.R., Fowler, W.A., 1988, At. Data Nucl. Data Tables, 40, 283
- Fujimoto, M.Y., Sugimoto, D., 1982, ApJ, 257, 767
- Hashimoto, M.-A., Nomoto, K.I., Arai, K., Kaminisi, K., 1984, Phys. Rep. Kumamoto Univ., 6, 75
- Hamuy, M., Phillips, M.M., Suntzeff, N.B., et al., 1996, ApJ, 519, 314
- Heber, U., Napiwotzki, R., Reid, I.N., 1997, A&A, 323, 819
- Heger, A., Langer, N., Woosley, S.E., 2000, ApJ, 528, 368
- Heger, A., Woosley, S., Langer, N., Spruit, H.C., 2003, in: Stellar Rotation, proc. IAU-Symp. 215, (San Francisco: ASP), A. Maeder, P. Eenens, eds., in press
- Maeder, A., Meynet, G., 2003, A&A, 411, 543

- Hillebrandt, W., Niemeyer, J.C., 2000, ARA&A, 38, 191
- Höflich, P., Khokhlov, A., 1996, ApJ, 457, 500
- Iben, I.Jr., Tutukov, A.V., 1991, ApJ 370, 615
- Kato, M., Hachisu, I., 2003, ApJ, 598, L107
- Kawaler S.D., 2003, in: Stellar Rotation, proc. IAU Symp. 215, A. Maeder, P. Eenens, eds.
- Koester, D., Dreizler, S., Weidemann, V., Allard, N.F., 1998, A&A, 338, 617
- Landau, L.D., Lifshitz, E.M., 1984, Fluid Mechanics, Course of theoretical physics, vol. 6, Pergamon Press
- Langer, N., 1998, A&A, 329,551
- Langer, N., Deutschmann, A., Wellstein, S., Höflich, P., 2000, A&A, 362, 1046
- Langer, N., Heger, A., Wellstein, S., Herwig, F., 1999, A&A, 346, L37
- Langer, N., Kiriakidis, M., El Eid, M.F., Fricke, K.J., Weiss, A., 1988, A&A, 192, 177
- Leibundgut, B., 2001, ARA&A, 39, 67
- Limongi, M., Tornambé, A., 1991, ApJ, 371, 317
- Livio, M., 2001, In: Cosmic evolution, ed. E. Vangioni, R. Ferlet, M. Lemoine, New Jersey: World Scientific
- Livne, E., 1990, ApJ, 354, L53
- Livne, E., Arnett, D., 1995, ApJ, 452, 62
- Maeder, A., Meynet, G., 2000, ARA&A, 38, 143
- Maeder, A., Meynet, G., 2003, A&A, 411, 543
- Mochkotvich, R., Livio, M., 1989, A&A, 209, 111
- Neo, S., Miyaji, S., Nomoto, K., Sugimoto, D., 1977, PASJ, 29, 249
- Nomoto, K., 1982, ApJ, 257, 780
- Nomoto, K., Thielemann, F.-K., Yokoi, K., 1984, ApJ, 286, 644
- Nugent, P., Baron, E., Branch, D., Fisher, A., Hauschildt, P.H., 1997, ApJ, 485, 812
- Paczyński B., 1991, ApJ 370, 597
- Phillips, M.M., 1993, ApJ, 413, L105
- Piersanti, L., Cassisi, S., Tornambé, A., 2001, ApJ, 558, 916
- Popham, R., Narayan, R., 1991, ApJ, 370, 604
- Regös, E., Tout, C.A., Wickramasinghe, D., Hurley, J.R., Pols, O.R., 2002, New Astron., 8, 283
- Renzini, A., 1999, In: Chemical Evolution from Zero to High Redshift, Heidelberg, Springer Verlag, 185
- Siess, L., Goriely, S., Langer, L., 2003, A&A, in press
- Taam, R.E., 1980, ApJ, 237, 142
- Woosley, S.E., Weaver, T.A., 1994, ApJ, 423, 371
- Yoon, S.-C., Langer, N., 2002, In: Physics of Cataclysmic Variables and Related Objects, ASP Conf. Proc. Ser. vol. 261, Ed. B.T. Gaensicke et al., p. 79
- Yoon, S.-C., Langer, N., 2004, A&A, accepted
- Yoon S.-C., Langer N., Scheithauer S., 2004, A&A, to be submitted